21. Oka T, Katayama K, Ogawa S, Hansman GS, Kageyama T, Ushijima H, Miyamura T, Takeda N (2005) Proteolytic processing of sapovirus ORF1 polyprotein. J Virol 79: 7283–7290
22. Okada M, Shinozaki K, Ogawa T, Kaiho I (2002) Molecular epidemiology and phylogenetic analysis of Sapporo-like viruses. Arch Virol 147: 1445–1451
23. Robinson S, Clarke IN, Vipond IB, Caul EO, Lambden PR (2002) Epidemiology of human Sapporo-like caliciviruses in the South West of England: molecular characterisation of a genetically distinct isolate. J Med Virol 67: 282–288
24. Schuffenecker I, Ando T, Thouvenot D, Lina B, Aymard M (2001) Genetic classification of "Sapporo-like viruses". Arch Virol 146: 2115–2132
25. Someya Y, Takeda N, Miyamura T (2000) Complete nucleotide sequence of the chiba virus genome and functional expression of the 3C-like protease in Escherichia coli. Virology 278: 490–500
26. Someya Y, Takeda N, Miyamura T (2002) Identification of active-site amino acid residues in the Chiba virus 3C- like protease. J Virol 76: 5949–5958
27. Sosnovtsev SV, Garfield M, Green KY (2002) Processing map and essential cleavage sites of the nonstructural polyprotein encoded by ORF1 of the feline calicivirus genome. J Virol 76: 7060–7072
28. Sosnovtseva SA, Sosnovtsev SV, Green KY (1999) Mapping of the feline calicivirus proteinase responsible for autocatalytic processing of the nonstructural polyprotein and identification of a stable proteinase-polymerase precursor protein. J Virol 73: 6626–6633
29. Wei L, Huhn JS, Mory A, Pathak HB, Sosnovtsev SV, Green KY, Cameron CE (2001) Proteinase-polymerase precursor as the active form of feline calicivirus RNA-dependent RNA polymerase. J Virol 75: 1211–1219
30. Wirblich C, Sibilia M, Boniotti MB, Rossi C, Thiel HJ, Meyers G (1995) 3C-like protease of rabbit hemorrhagic disease virus: identification of cleavage sites in the ORF1 polyprotein and analysis of cleavage specificity. J Virol 69: 7159–7168
31. Wirblich C, Thiel HJ, Meyers G (1996) Genetic map of the calicivirus rabbit hemorrhagic disease virus as deduced from in vitro translation studies. J Virol 70: 7974–7983

Author's address: Tomoichiro Oka, Department of Virology II, National Institute of Infectious Diseases, Gakuen 4-7-1, Musashi-murayama, Tokyo 208-0011, Japan; e-mail: oka-t@nih.go.jp

Arch Virol (2006) 151: 1291–1308
DOI 10.1007/s00705-005-0720-9

Archives of Virology
Printed in Austria

Investigation of norovirus replication in a human cell line

K. Katayama, G. S. Hansman, T. Oka, S. Ogawa, and **N. Takeda**

Department of Virology II, National Institute of Infectious Diseases, Tokyo, Japan

Received July 5, 2005; accepted December 21, 2005
Published online February 26, 2006

Summary. Noroviruses (NoVs) belong to the genus *Norovirus* and are members of the family *Caliciviridae*. NoVs are the dominant cause of outbreaks of gastroenteritis, but progress in understanding the molecular characteristics of NoV and its replication strategies have been hampered by the lack of a cell culture system or a practical animal model, except for murine NoVs. To elucidate the transcription and replication of the NoV genome, a complete genome of a human NoV genogroup II strain was cloned downstream of a T7 RNA polymerase promoter and expressed in human embryonic kidney (HEK) 293T/17 cells using a T7 vaccinia virus expression system. Bands for a 7.6-kb negative-strand RNA, a 7.6-kb positive-strand genomic RNA, and a 2.6-kb positive-strand subgenomic-like RNA were found in the infected cells. However, recombinant capsid protein (rVP1) and rVP2 were not detected by Western blotting. When a construct containing VP1 and VP2 genes was co-transfected with a full-length construct, the expression of virus-like particles (VLPs) with a buoyant density of 1.271 g/cm^3 was observed. We also observed round particles, 20 to 80 nm in diameter, with a buoyant density of 1.318 g/cm^3. Our results indicated that NoV RNA was incorporated into the heavier particles. However, further studies are needed to investigate the antigenicity of these particles and to determine if they represent undeveloped VLPs.

Introduction

Noroviruses (NoVs) belong to the genus *Norovirus* and are members of the family *Caliciviridae*. NoVs are the dominant cause of outbreaks of gastroenteritis worldwide, usually via the contamination of foods such as oysters, shellfish, ice, and person-to-person transmission [18, 24]. Although the symptoms, which include nausea, vomiting, and diarrhea, are self-limiting, infected children may be hospitalized and require the use of intravenous therapy [10, 11]. As such, a vaccine for NoV has been developed but has yet to be approved [1, 2].

The NoV genome consists of a positive-sense, single-stranded RNA of approximately 7.6 kb in length that is organized in three open reading frames (ORFs).

Open reading frame 1 (ORF1) encodes non-structural proteins, including N-terminal protein (N-term), NTPase, 3A-like protein (3A-like), genome-linked viral protein (VPg), 3C-like protease (Pro), and RNA-dependent RNA polymerase (RdRp). ORF2 encodes the major capsid protein (VP1), and ORF3 encodes a small protein (VP2) associated with VP1 stability. To date, all laboratory efforts to cultivate human NoV have failed [7], but expression of the recombinant VP1 (rVP1) in insect or mammalian cells can result in the formation of virus-like particles (VLPs) that are morphologically similar to native NoV [3, 5, 13, 14, 16, 28, 31]. These studies have provided valuable information, including the high-resolution atomic structure and information on antigenicity among the strains and binding factors. However, it remains unclear how similar these VLPs are to native NoV [27]. In recent studies murine NoV was successfully cultured in cultured dendritic cells and macrophages, providing the first model for a NoV [19, 33].

The three other genera of the family *Caliciviridae* are *Sapovirus*, *Lagovirus*, and *Vesivirus*, which include sapovirus (SaV), rabbit hemorrhagic disease virus (RHDV), and feline calicivirus (FCV) strains, respectively. Porcine SaV (PEC strain) and FCV can be grown in culture systems, although after the PEC strain was adapted to cell culture, several amino acid substitutions in the genome were detected [8, 26, 30].

The purpose of this study was to express human NoV in cultured human embryonic kidney (HEK) 293T/17 cells using a number of different constructs, including a full-length construct (pT7U201F) that was designed to produce RNA identical to the genomic RNA and a construct with only ORF2 and ORF3 genes (pT7U201-ORF23), which could be analogous to the subgenomic RNA.

Materials and methods

Design of expression constructs

NoV strain U201 (accession number AB067542) was isolated from an outbreak of gastroenteritis in 1998 [20]. The U201 strain belonged to NoV genogroup II (GII/3; Mexico cluster), and the full-length sequence was determined. To develop the expression constructs we extracted the RNA as previously described [20]. All amplifications were performed using KOD Plus polymerase (Toyobo, Osaka, Japan), and the primers are listed in Table 1. cDNA was synthesized with Tx30SXN primer and Superscript III reverse transcriptase according to the manufacturer's instructions (Invitrogen, Carlsbad, CA). A single PCR fragment of 7.6 kb was amplified with sense primer U201-1S30 and antisense primer Tx30SXN, and then cloned into pCR-Blunt-II-TOPO vector (Invitrogen). This plasmid was designated pCR-Blunt-U201-F, which contained the full-length genome of U201. Several amplification and cloning steps were performed in order to produce a full-length expression construct having a T7 RNA polymerase promoter at the 5′ end and an HDV ribozyme and a T7 terminator at the 3′ end. Briefly, the 5′ end of pCR-Blunt-U201-F was amplified with sense primer NKT7-U201-1S30 and antisense primer U201-3852A. This fragment was digested with *Not*I and *Nde*I restriction enzymes; the corresponding fragment was termed I (U201 contained a unique *Nde*I site at position 3538). Next, we amplified the 3′ end of pCR-Blunt-U201-F plasmid with sense primer U201-6405S and antisense primer Ribo24-Tx30-U201end23A; the corresponding fragment was termed II. We then amplified HDV ribozyme and T7 terminator sequences from the pT7HCV09Luc plasmid [34] with sense primer Ribo1S24 and antisense

Table 1. Primers used to design the constructs

Name	Sequence (5′ to 3′)	Description
Tx30SXN	GACTAGTTCTAGATCGCGAGCGGCCGCCC TTTTTTTTTTTTTTTTTTTTTTTTTTTTT	RT-PCR
U201-1S30	GTGAATGAAGATGGCGTCTAACGACGCTTC	Amplification
NKT7-U201-1S30	AATCGAATTCAAGCGGCCGCGGTACCGCGG CCGCGGTACC TAATACGACTCACTATA GTGAATGAAGATGGCGTCTAACGACGCTTC	*Not*I and *Kpn*I restriction enzyme sites (underlined) and a T7 promoter site (double underlined)
U201-3852A	CCCTCAAGAGTGGCTTCACCTTCG	Amplification
U201-6405S	CAGCTACTTTTCTTCCGATCACAGCTG	Amplification
Ribo24-Tx30-U201end23A	GAGGTGGAGATGCCATGCCGACCCTTTTT TTTTTTTTTTTTTTTTTTTTTTTTAAAA GATTCTAAATCAAATTTAG	24 nucleotides of the HDV ribozyme sequence (underlined)
Ribo1S24	GGGTCGGCATGGCATCTCCACCTC	Amplification
T7term-MluAsc-A	AGGCGCGCGCCACGCGTTCCTTTCAGCAA AAAACCCCTCAAG	*Mlu*I site restriction enzyme (underlined)
MUTforward	TAGGCACAACACCAGGTGACgGTGGGTGCC	Mutagenesis (change from c to g)
MUTreverse	GTCACCTGGTGTTGTGCCTAGGTCCATGCT	Mutagenesis
ORF2forward	GGGGTACC TAATACGACTCACTATAGGGGT GAATGAAGATGGCGTCGAATGACGCTG	*Kpn*I restriction enzyme site (underlined) and a T7 promoter site (double underlined)
ORF3forward	GGGGTACC TAATACGACTCACTATAGGGGATT CAATAATGGCTGGAGCTTTTATAGCAGG	*Kpn*I enzyme site (underlined) and a T7 promoter (double underlined)
U201-5051S	CATGGGAGGGCGATCGCAA	Detection of RNA
U201-5391A	CCTGCATAACCATTGTACAT	Detection of RNA

primer T7term-MluAsc-A; the corresponding fragment was termed III. After fragments II and III were joined in a primer-less PCR (using the 24-base overlap in primer Ribo24-Tx30-U201end23A), we digested the 5′ and 3′ ends with *Pfl*MI and *Mlu*I restriction enzymes; the corresponding fragment was termed IV. Next, pCR-Blunt-U201F was digested with *Not*I and cloned into a previously *Not*I-digested modified pMT1 vector. Since this vector is a low-copy plasmid, the number of nucleotide mutations would be reduced when expressed [22]; the corresponding plasmid was termed pT7U201F/MT1. Next, pT7U201F/MT1 was digested with *Kpn*I and *Nde*I restriction enzymes and fragment I was inserted; the corresponding plasmid was termed pT7U201F/MT1 + I, which contained the full-length U201 and a T7 promoter at the 5′ end. Plasmid pT7U201F/MT1 + I was digested with *Pfl*MI and *Mlu*I restriction enzymes and fragment IV was inserted; the corresponding plasmid was termed pT7U201F, which contained a T7 promoter at the 5′ end and an HDV ribozyme and a T7 terminator at the 3′ end. This plasmid (pT7U201F) is able to generate the full-length U201 RNA when bacteriophage T7 RNA polymerase is provided. The pT7U201F also served as a template for the development of four other NoV expression constructs. We designed a second full-length construct with a mutation in the protease "GDCG" motif (termed pT7U201F-Pro/m) in which an amino acid residue was changed from GDCG to GDGG (shown in bold), thus generating polyproteins with no protease activity. This was accomplished using

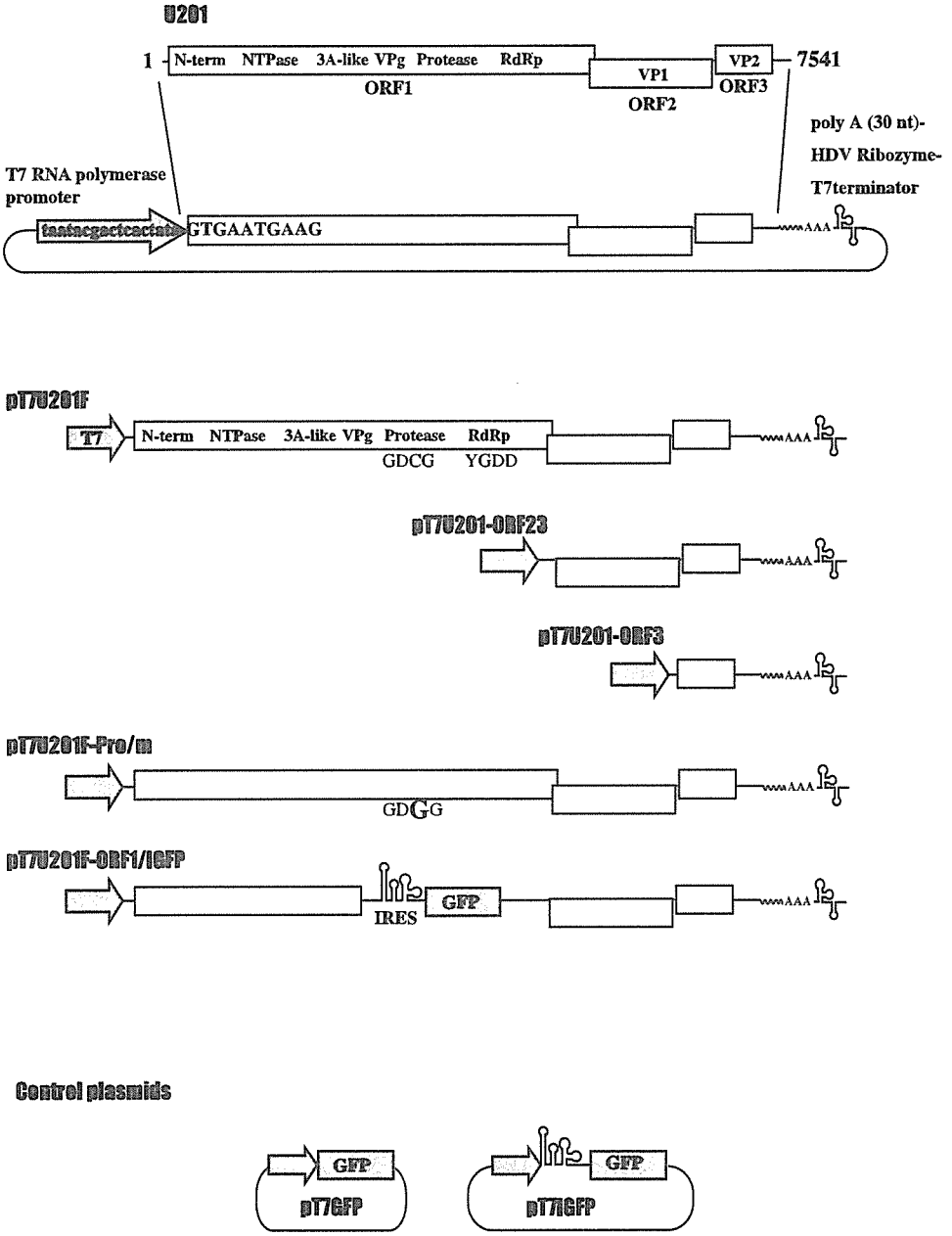

Fig. 1. The genomic organization of the NoV U201 strain, indicating the positions of the ORF1 genes (N-term, NTPase, 3A-like, VPg, Protease, and RdRp), the ORF2 gene (VP1), and the ORF3 gene (VP2). The schematics of the expression constructs are based on the genomic organization of U201: pT7U201F (genomic-like-RNA); pT7U201-ORF23 (subgenomic-like-RNA); pT7U201-ORF3 (VP2 gene only); pT7U201F-Pro/m (mutated-protease gene); pT7U201-ORF1/IGFP (disrupted RdRp gene); pT7GFP (GFP control); and pT7IGFP (IGFP control)

a Genetailor site directed mutagenesis kit (Invitrogen) with sense primer MUTforward and antisense primer MUTreverse. We designed a third full-length construct with an EMCV-IRES and a GFP gene (termed pT7U201F-ORF1/IGFP), which was from the pIRES2-EGFP plasmid (Clontech, Palo Alto, CA). In this construct, the RdRp region (nucleotide position 2518 to 3859) was disrupted using *Xho*I and *Xba*I sites, so that an IRES-dependent GFP signal was detectable when RNA was generated by T7 RNA polymerase. We designed a construct with only ORF2 and ORF3. For this construct, the region from ORF2 to the 3′ end of the genome was amplified with sense primer ORF2forward and antisense primer T7term-MluAsc-A. This fragment was cloned into modified pMT1 using the *Kpn*I and *Mlu*I site; the corresponding plasmid was termed pU201-ORF23. We designed a construct with only ORF3. For this construct, the region from ORF3 to the 3′ end of the genome was amplified with sense primer ORF3forward and antisense primer T7term-MluAsc-A. This fragment was cloned into modified pMT1; the corresponding plasmid was termed pT7U201-ORF3. All NoV constructs had a T7 RNA polymerase promoter at the 5′ end, whereas at the 3′ end, all constructs had a poly(A) tail, an HDV ribozyme, and a T7 terminator (Fig. 1). We also designed two control plasmids to monitor either cap-dependent or cap-independent translation of EGFP (EGFP and IRES-EGFP, respectively). EGFP and IRES-EGFP were amplified from pIRES2-EGFP and cut out with restriction enzymes. After a blunt-end reaction, the EGFP and IRES-EGFP fragments were cloned into pGEM4Z plasmid; the corresponding plasmids were termed pT7GFP and pT7IGFP, respectively. All clones were confirmed by sequencing.

Cells and expression of constructs

The human embryonic kidney (HEK) 293T/17 cells (293T) were purchased from the American Type Culture Collection, Rockville, MD, and maintained in Dulbecco's minimum essential medium (DMEM) containing penicillin (250 U/ml), streptomycin (250 μg/ml), and 10% heat-inactivated fetal bovine serum (FBS) (Invitrogen). Two days before the superinfection, 2.0×10^5 cells were put into a 35 mm dish and were grown in DMEM. The vTF7, a vaccinia virus recombinant that expresses the T7 polymerase (kindly provided by Bernard Moss, National Institutes of Health, Bethesda), was propagated as previously described [29]. 293T cells were infected with vTF7 at room temperature for 1 h at a multiplicity of infection (MOI) of 0.1. After infection, transfection of plasmid(s) was performed with Effectene transfection reagent as recommended by the supplier (QIAGEN, Valencia, CA).

Purification of VLPs

The culture medium and cells were harvested at 6, 12, 24, 48, and 72 h post-infection (hpi). The culture medium was collected and centrifuged for 10 min at $3{,}000 \times g$, and then further centrifuged for 1 h at $20{,}000 \times g$. The proteins in the supernatant were precipitated by ultracentrifugation for 3 h at 30,000 rpm (Beckman SW32Ti rotor) and resuspended in OptiMEM serum-free medium (Invitrogen). The cells were removed with a cell scraper and resuspended in OptiMEM medium. The proteins in the cells were released by freeze/thawing (three times) and then prepared as described above.

SDS-PAGE, Western blotting, Northern blotting, electron microscopy, and RT-PCR

A panel of antibodies specific for NoV non-structural proteins, consisting of N-term, NTPase, 3A-like, VPg, Pro, and RdRp, was prepared as described previously [25]. SDS-PAGE, Western blotting, Northern blotting, and electron microscopy (EM) were performed as described previously [12]. RNA was extracted from the VLPs using Isogen solution (WAKO, Osaka,

Japan) and was detected with the U201-specific sense primer U201-5051S and antisense primer U201-5391A as described previously [17, 21].

Large-scale expression of VP1

Four 6-well culture plates were used for large-scale expression of VLPs with vTF7 superinfection. The cultured cells were transfected with pT7U201F and pT7U201-ORF23 and then harvested at 48 hpi. VLPs were purified as described above but resuspended in 100 μl OptiMEM, followed by CsCl equilibrium gradient ultracentrifugation (1.34 g/cm^3) for 40 h at 45,000 rpm at 10 °C (Beckman SW-55Ti rotor). Two hundred microliters was collected from the bottom of the tube (22 fractions in total). Each fraction was concentrated for 3 h at 50,000 rpm (Beckman 55Ti rotor) and then resuspended in 20 μl of OptiMEM and treated with RQ1 DNase and RNase A (Sigma, St. Louis, MO).

Immunofluorescence analysis

293T cells grown in 4-well tissue culture plates were infected with vTF7, transfected with plasmid DNA, and then fixed with 4% paraformaldehyde (PFA) at 6, 12, 24, 48, and 72 hpi for immunofluorescent (IF) staining. Cells were permeabilized in 0.1% Triton X-100 for 10 min prior to the addition of the antibodies. Following washing with PBS (pH 7.4), purified rabbit IgG fraction specific for the VP1 (dilution 1:4,000) or anti-VPg monoclonal antibody (MoAb) (1 μg/ml; which was produced by *E. coli* expressed recombinant GST tagged fusion VPg protein, following the position at anti-VPg MoAb) was added and incubated at room temperature between 3 and 12 h at 4 °C. The wells were washed three times with PBS, and fluorescein isothiocyanate (FITC)-conjugated, affinity-purified goat antibody to rabbit IgG (dilution 1:20) (Invitrogen) was added in order to detect the primary VP1 antibody. To detect anti-VPg MoAb, affinity-purified Alexa Fluor 568-labeled goat antibody to mouse IgG (dilution 1:200) (Invitrogen) was used. For detection of primary antibody binding, slides were incubated in the dark for 1 h with FITC-labeled, affinity purified Alexa Fluor 568-labeled goat antibodies to guinea pig IgG (1:200) (Invitrogen). In addition, 4,6-diamidino-2-phenylindole dihydrochloride hydrate (DAPI) (Invitrogen) was used for staining of the nuclei. The slides were washed twice with PBS and then once with distilled water. One drop of antifade reagent-mounting mixture (Invitrogen) was placed on the center of each slide after staining, a coverslip was added, and the mounting agent was allowed to dry. After sealing, the slides were stored at room temperature. Images were collected using a 63 water immersion objective, zoom 1 or 2, on a Zeiss LSM 510 confocal microscope (Carl Zeiss, Jena, Germany) by argon-krypton laser excitation at 488 nm for FITC (green) and 568 nm for Alexa-Fluor (red). The UV fluorescence for DAPI (blue) was excited using an argon laser (364 nm). The images were analyzed in Adobe Photoshop (Adobe Systems Incorporated, San Jose, CA).

Results

Expression in 293T cells

The expression of the NoV constructs in 293T cells was analyzed with a panel of purified rabbit IgG antisera that were raised against *E. coli*-expressed recombinant ORF1-encoded proteins: rN-term (amino acids 1–169 of the ORF1), rNTPase (amino acids 488–699), r3A-like (amino acids 702–878), rVPg (amino acids 879–1011), rPro (amino acids 1012–1192), and rRdRp (amino acids 1193–1707), rVP1 (complete length of the ORF2), and rVP2 (complete length of the ORF3). Samples were collected at 6, 12, 24, 48, and 72 hpi, and equal volumes were

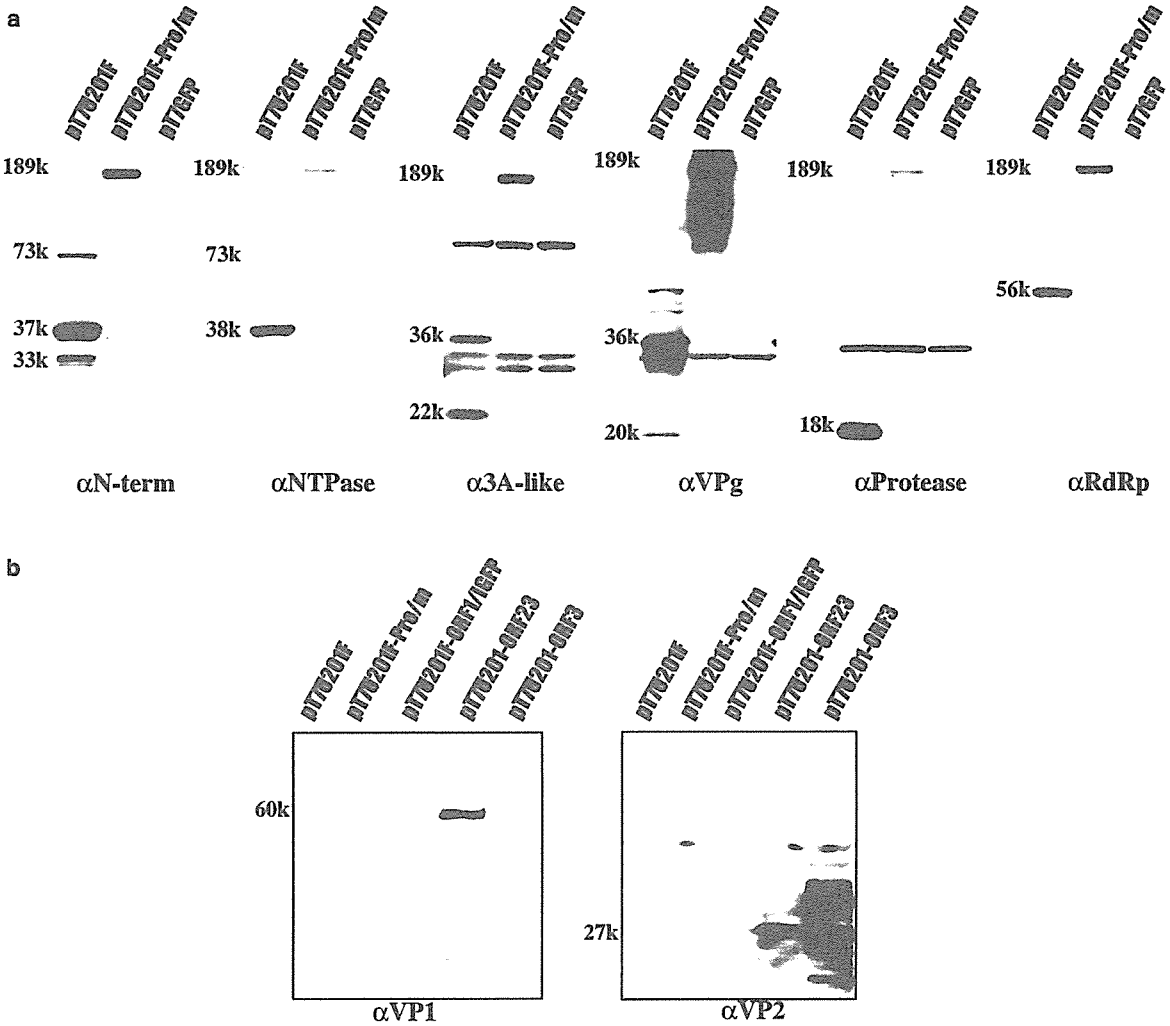

Fig. 2. Expression of NoV constructs was analyzed by antisera that were raised against the *E. coli*-expressed ORF1 proteins (N-term, NTPase, 3A-like, VPg, protease, and RdRp), the ORF2 protein (VP1), and the ORF3 protein (VP2), corresponding to 37, 38, 22, 20, 18, 56, 60, and 27 kDa, respectively. Equal volumes of samples collected 24 hpi were loaded into separate wells of a 5–20% gradient polyacrylamide gel. All ORF1 proteins were detected with the pT7U201F construct. A single polyprotein of 189 kDa was detected for the pT7U201F-Pro/m construct. The control pT7U201F-ORF1/IGFP construct showed no signals against any of these antibodies

loaded into separate wells of a 5–20% gradient polyacrylamide gel. For the full-length construct (pT7U201F), each of the ORF1-encoded proteins, i.e., rN-term, rNTPase, r3A-like, rVPg, rPro, and rRdRp was detected, as 37-kDa, 38-kDa, 22-kDa, 20-kDa, 18-kDa, and 56-kDa bands, respectively (Fig. 2, shown at 24 hpi). For the mutated-protease construct (pT7U201-F-Pro/m), a single polyprotein of 189 kDa, which corresponded to the estimated product size of the ORF1-encoded

polyprotein, was detected with the N-term, NTPase, 3A-like, VPg, Pro, and RdRp antisera. The control GFP pT7GFP construct showed no signals against any of these antibodies (data not shown). These results indicated that the ORF1-encoded protein was cleaved by the viral protease, since cleaved ORF1 proteins were not detected with the mutated-protease construct (Fig. 2a). Western blot analysis also revealed several precursor proteins with the pT7U201F construct. A precursor protein of 73 kDa was detected with the N-term and NTPase antisera; however, the 73-kDa band intensities were weaker than those of the rN-term and rNTPase proteins (37 and 38 kDa, respectively). A 33-kDa band detected with the N-term antisera was not further characterized in this study. Precursor protein bands of 36 kDa were detected with the 3A-like and VPg antisera. The band intensity of the 36-kDa and r3A-like (22-kDa) proteins were similar, whereas the band intensity of the 36-kDa protein was greater than that of the rVPg protein (20 kDa). Surprisingly, matured products appeared weakly at 6 hpi, and then the signal intensity increased over time, except in the case of r3A-like and rVPg (data not shown). In particular, the rPro-RdRp precursor was not detected in our system. These results suggested that cleavage of the 36 kDa precursor protein was slower than that of the 73-kDa precursor protein.

The rVP1 was only expressed with the pT7U201-ORF23 construct, as seen by the band of 60 kDa. The rVP2 was expressed with both the pT7U201-ORF23 and pT7U201-ORF3 constructs, as seen by the bands of 27 kDa (Fig. 2b). Neither rVP1 nor rVP2 was detected with the pT7U201F construct. Following these results, we

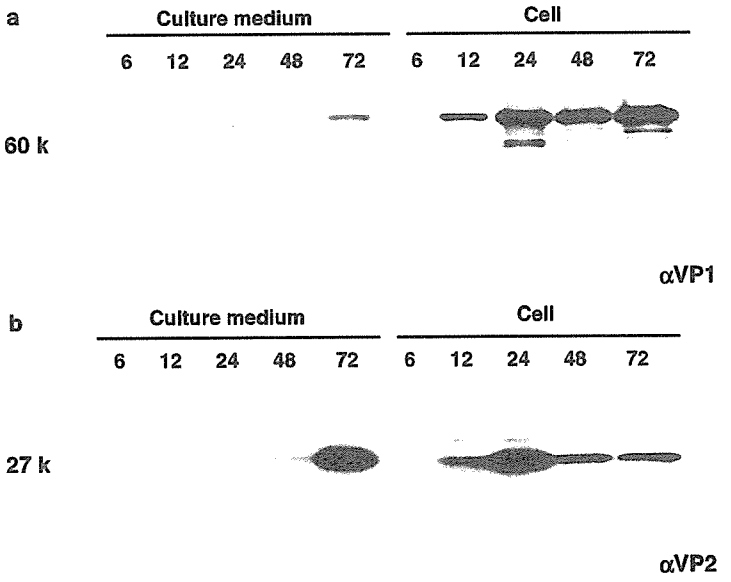

Fig. 3. The time-course expression of VP1 and VP2 in the cell lysate and culture medium that were stained at 6, 12, 24, 48, and 72 hpi. **a** VP1 was observed in the cell lysate from 12 hpi, whereas VP1 was only detected in the culture medium at 72 hpi. **b** VP2 was observed in the cell lysate and culture medium, but the exposure time was 15 min for VP2, compared to 15 s for VP1, which indicates that the translation of VP1 was faster and more efficient than that of VP2

co-transfected pT7U201F and pT7U201-ORF23 and examined the time-course expression of rVP1 and rVP2 in the cell lysate and culture medium (Fig. 3a and b). Samples were stained at 6, 12, 24, 48, and 72 hpi. The rVP1 was observed in the

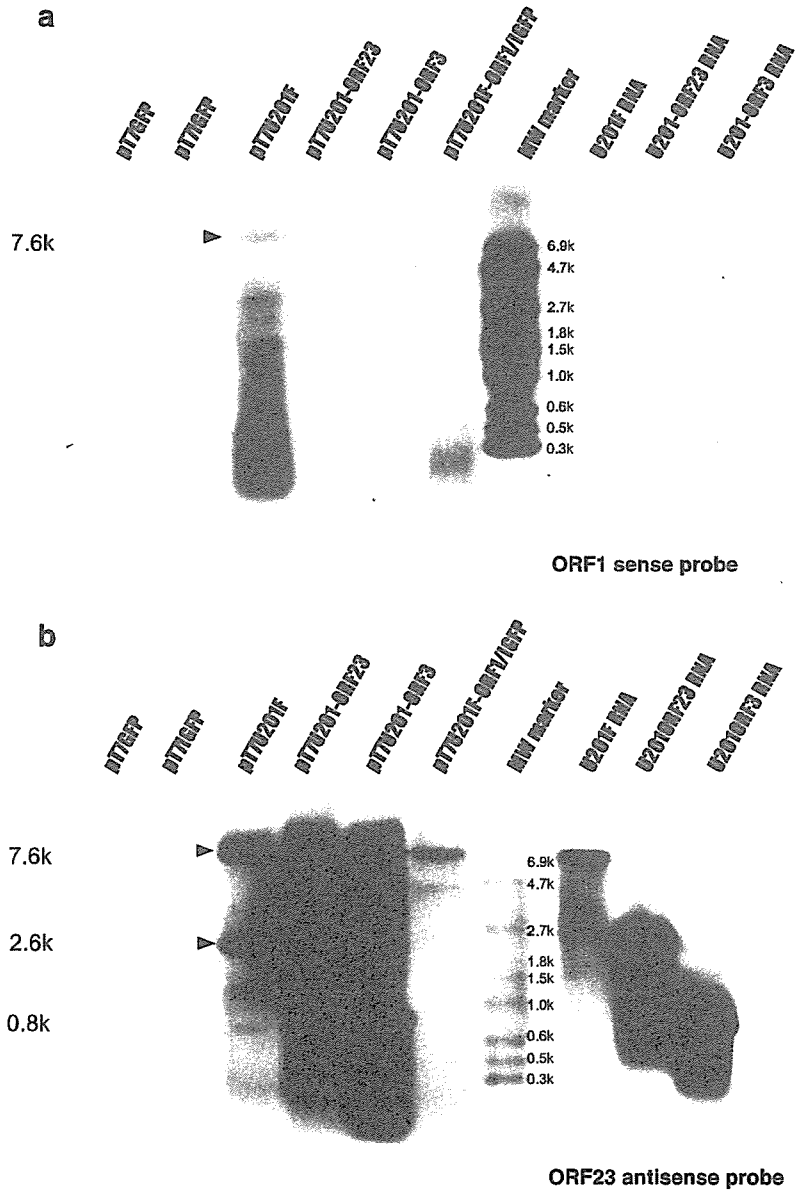

Fig. 4. Total RNA was extracted from the cells and analyzed by Northern blotting. **a** A full-length negative-strand RNA was detected with the pT7U201F construct (7.6 kb). **b** Positive-strand full-length RNA (7.6 kb) and positive-strand subgenomic RNA (2.6 kb) were detected with the pT7U201F construct; a positive-strand 2.6-kb RNA band was detected with the pT7U201-ORF23 construct; a 0.8-kb band was detected with the pT7U201-ORF3 construct; and a 7.6-kb band was detected with the pT7U201F-ORF1/IGFP construct

cell lysate at 12 hpi and was constantly synthesized thereafter. The rVP1 was only detected in the culture medium at 72 hpi, at which time most of the cells appeared broken. The rVP2 was similarly observed in the cell lysate and culture medium, but the exposure time was 15 min for rVP2 compared to 15 s for rVP1. This result indicated that the translation of rVP1 was faster and more efficient than that of rVP2.

Northern blot analysis

Total RNA was extracted from the cells and analyzed by Northern blotting. A negative-strand genomic-like RNA band (7.6 kb) was detected with the full-length construct (Fig. 4a). In contrast, a negative-strand genomic-like RNA band was not detected with the construct that had a disrupted RdRp (pT7U201F-ORF1/IGFP). A negative-strand genomic-like RNA band was not detected with any of the control constructs. These data indicated that functional RdRp was generated, and the negative-strand genomic-like RNA was synthesized from the positive-strand genomic-like RNA. A positive-strand subgenomic-like RNA band (2.6 kb) was detected with the subgenomic-like construct (pT7U201-ORF23) and was similar in size to that of the positive-strand subgenomic-like RNA band (2.6 kb) derived with the full-length construct (Fig. 4b). A positive-strand genomic-like RNA band (7.6 kb) was also detected with the pT7U201F-ORF1/IGFP construct. The 2.6-kb band was not detected with the pT7U201F-ORF1/IGFP construct. These results indicated that the viral RdRp produced the subgenomic-like RNA. The positive-strand genomic-like RNA of the pT7U201F construct was not only synthesized from vTF7, providing T7 RNA polymerase, but was also synthesized by RdRp, which was provided from pT7U201F. The ORF3 construct (pT7U201-ORF3) produced a band of 0.8 kb (Fig. 4b), i.e. the expected size of the VP2 gene. All signals disappeared when treated with DNase-free RNase A before Northern blotting.

Immunofluorescence analysis

The time-course expression of both the pT7U201F and pT7U201-ORF23 constructs was analyzed by immunofluorescence using anti-VPg MoAb and anti-VP1 purified rabbit IgG. Samples were stained at 6, 12, 24, 48, and 72 hpi. For the pT7U201-ORF23 construct, green rVP1 signals were detected in the cytoplasm from 6 to 72 hpi. The intensity of green signals became stronger over time (Fig. 5a). For the pT7U201F construct, only red rVPg signals near the nucleus were detected, and the intensity of these signals increased over time. We did not detect any green rVP1 signals for the pT7U201F construct (Fig. 5b). The time-course expression of co-transfected pT7U201F and pT7U201-ORF23 constructs was also examined with anti-VP1 and -VP2 purified rabbit IgG (Fig. 6). Samples were stained at 24, 48, and 72 hpi. The rVP1 and rVP2 were detected as green and red signals, respectively. The results suggested that expression of rVP1 was faster than that of rVP2. VP1 appeared to localize within the cytoplasm at 24, 48, and 72 hpi. At 48 hpi, rVP2 aggregated and appeared in granule-like forms, whereas at 72 hpi, rVP2 spread and co-localized with rVP1 within the cytoplasm.

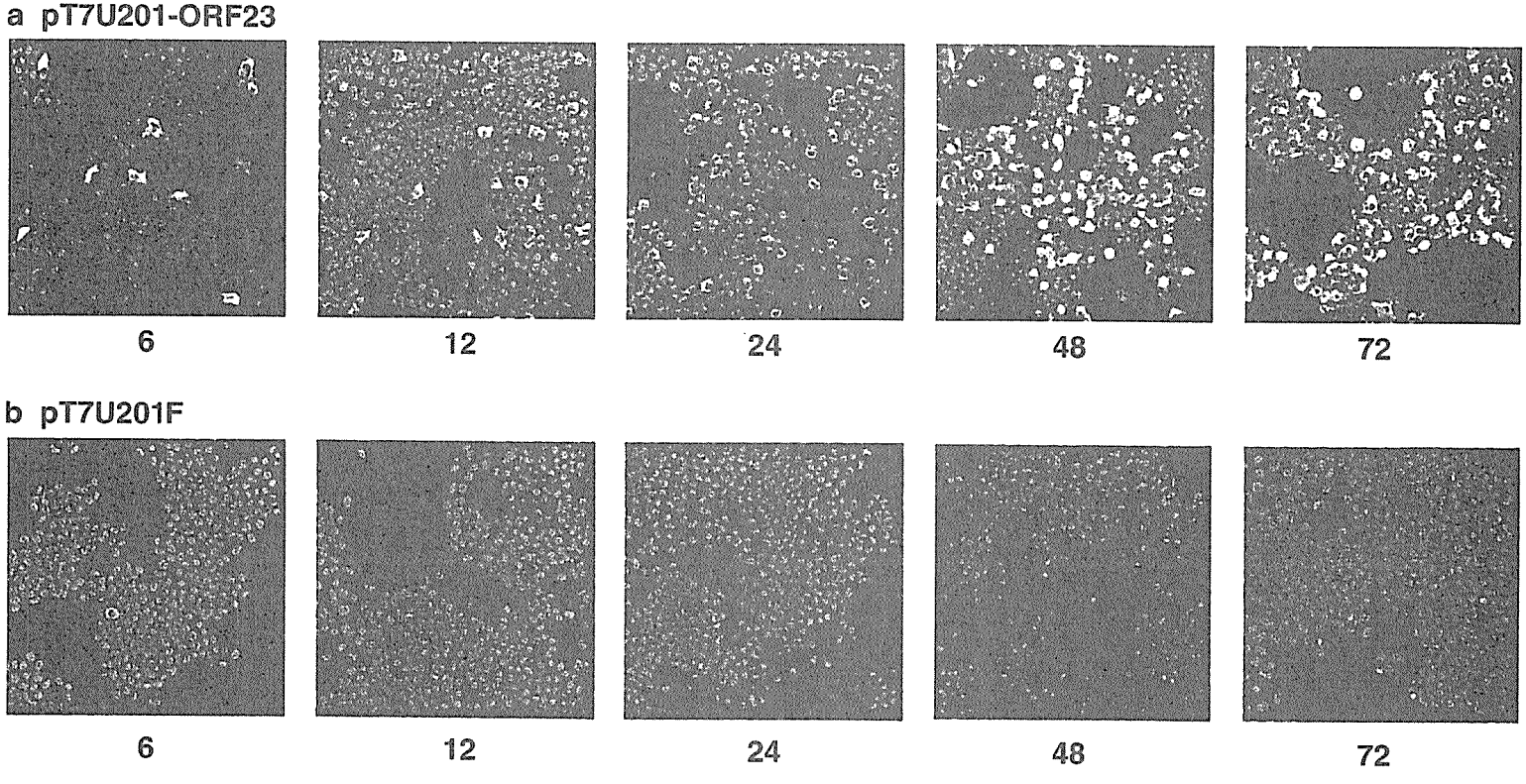

Fig. 5. The time-course expression of (**a**) pT7U201-ORF23 and (**b**) pT7U201F was analyzed by immunofluorescence with anti-VPg MoAb and anti-VP1 purified rabbit IgG. Samples were stained at 6, 12, 24, 48, and 72 hpi. For the pT7U201-ORF23 construct, green VP1 signals were detected in the cytoplasm from 6 to 72 hpi, and became stronger over time. For the pT7U201F construct, only red VPg signals near the nucleus were detected, and the intensity of these signals increased over time

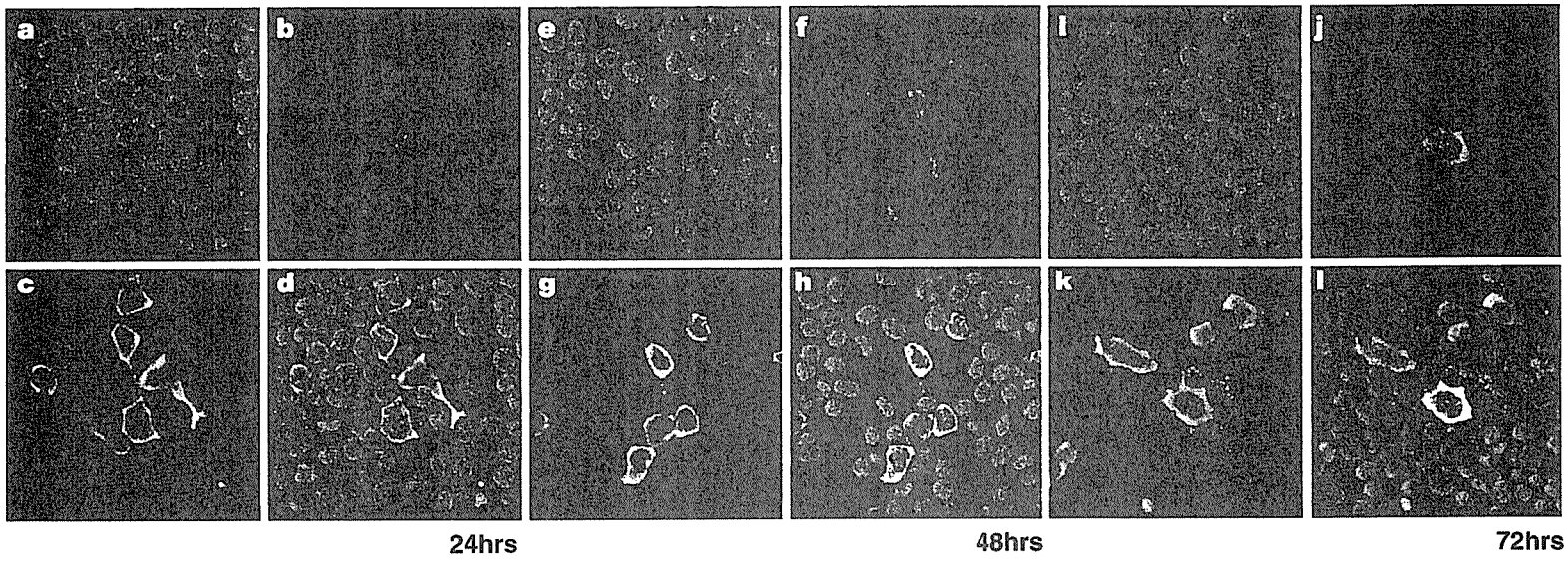

Fig. 6. The time-course expression of co-transfected pT7U201F and pT7U201-ORF23 constructs was examined with anti-VP1 and -VP2 purified rabbit IgG. Samples were stained at 24, 48, and 72 hpi. VP1 (green) and VP2 (red). A control was used throughout the experiment, i.e. no antibody (**a**, **e**, and **i**); only VP2 antibody (**b**, **f**, and **j**); only VP1 antibody (**c**, **g**, and **k**); and both VP1 and VP2 antibodies (**d**, **h**, and **l**). Expression of VP1 appeared more quickly than that of VP2. VP1 appeared to localize within the cytoplasm at 24, 48, and 72 hpi, whereas VP2 aggregated and appeared in granule-like forms at 48 hpi, and then spread and co-localized with VP1 within the cytoplasm at 72 hpi

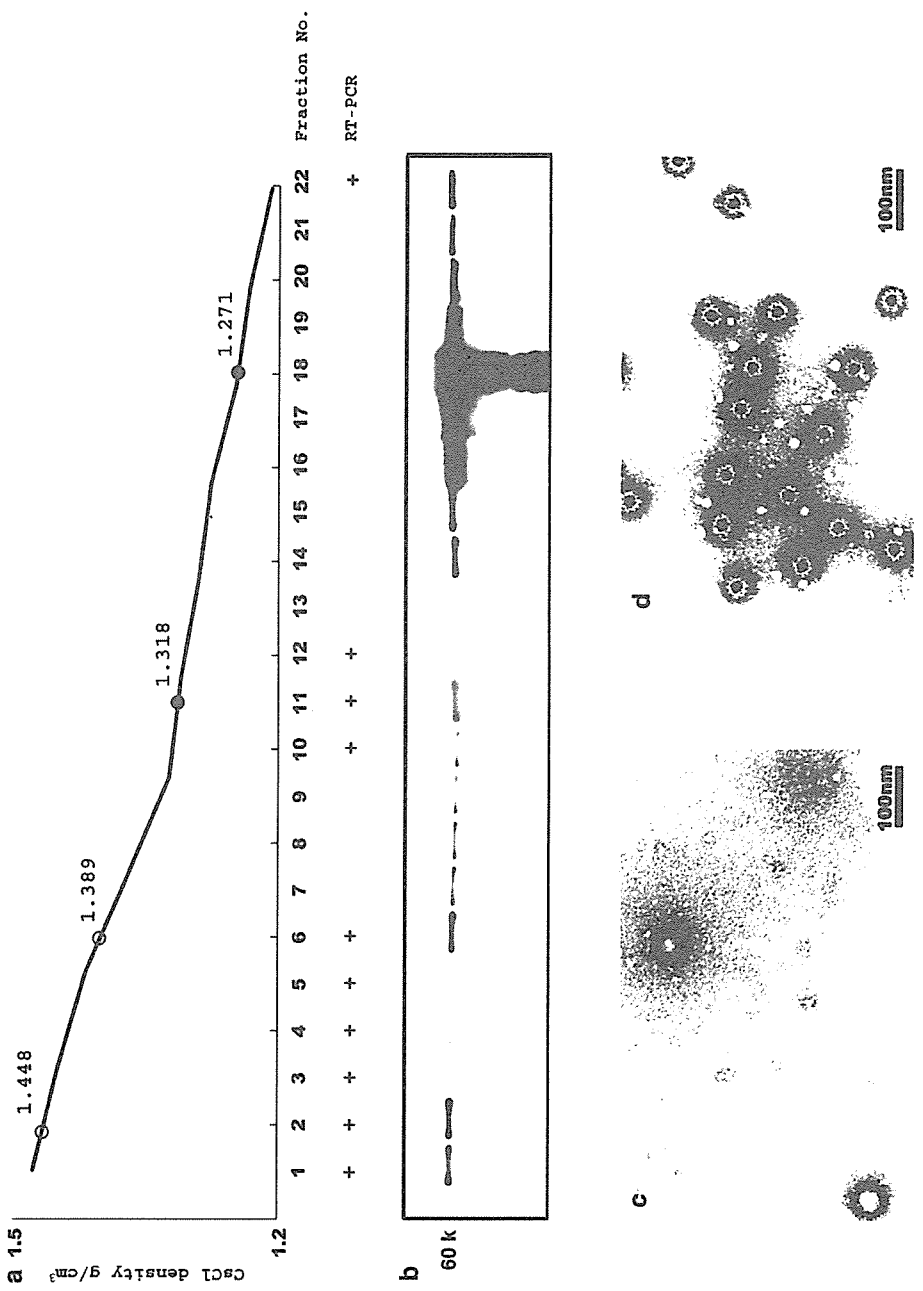

Fig. 7. Twenty-two fractions were collected from CsCl buoyant density centrifugation as described in Materials and methods, Large-scale expression of VP1 section. **a** The densities of the fractions were plotted. The open circles indicate the density of native NoV, the closed circles indicate the density of the VLPs detected in this study, and the plus signs represent positive RT-PCR fractions. **b** Western blotting of the 22 fractions using anti-VLP antisera. **c** The EM photo of fraction 11 (1.318 g/cm^3). **d** The EM photo of fraction 18 (1.271 g/cm^3). The solid black line indicates 100 nm

EM, RT-PCR, CsCl sedimentation, and Western blotting

As described above, the pT7U201F construct could provide the 7.6-kb negative strand genomic-like RNA, the 7.6-kb positive-strand genomic-like RNA, and the 2.6-kb positive subgenomic-like RNA. This construct could also express ORF1 non-structural proteins. However, our results showed that the full-length construct failed to express rVP1 and rVP2 proteins. In order to overcome this problem and to see whether VLP formation occurred, we co-transfected pT7U201F and pT7U201-ORF23 constructs, since the pT7U201-ORF23 construct was found to express rVP1 and rVP2 proteins and form VLPs (data not shown). The cell lysate was purified and analyzed by CsCl buoyant density centrifugation (Fig. 7a). Twenty-two fractions were collected and examined by single-round RT-PCR using U201 capsid region-specific primers, Western blotting, and EM (Fig. 7). Fractions 1 to 6 and 10 to 12 were positive by RT-PCR (Fig. 7a). Fraction 22 was also positive by RT-PCR, but likely included cell-associated or lipid-associated NoV RNA. Fractions 1 to 12 and 14 to 22 were positive for the 60-kDa rVP1 proteins by Western blotting (Fig. 7b). Fraction 18 (1.271 g/cm^3) showed the greatest band intensity but also included many degraded proteins. This density was slightly less than that of U201 VLPs expressed in insect cells (1.30 g/cm^3; and data not shown). Fractions 1, 2, 6 (less than 1.389 g/cm^3), and 11 (1.318 g/cm^3) had intermediate-strength rVP1 protein band intensities but were also positive by RT-PCR. Interestingly, fractions between 2 and 6 corresponded to the native NoV density. However, fractions 1, 2, and 6 contained only aggregated matter (data not shown). Fraction 11 (1.318 g/cm^3) contained round particles that ranged in size between 20 and 80 nm (Fig. 7c). Fraction 18 contained many VLPs that were morphologically similar to insect cell-expressed NoV VLPs (Fig. 7d).

Discussion

In order to better understand host infection factors, a model that closely mimics the natural host infection is required. To date, all laboratory efforts to cultivate human NoV strains have failed [7]. Nevertheless, expression of human NoV in insect or mammalian cells results in the formation of empty VLPs (i.e., without NoV nucleic acid) that are antigenically and morphologically similar to native NoV. Development of a self-replicating complete NoV VLP (i.e., containing RNA) would greatly enhance our understanding of NoV infectivity, antigenicity, and binding factors. The purpose of this study was to investigate NoV replication in a human cell line and produce an infectious artificial NoV particle.

The human NoV U201 strain was expressed in human 293T cells using a number of different constructs. Our results showed that ORF1-encoded proteins, i.e., rN-terminal protein (p37), rNTPase (p38), r3C-like protease (p18), and rRdRp (p56), were cleaved by the viral protease. These proteins were not detected with a mutated-protease construct (Fig. 2). The cleavage of the 189-kDa precursor protein was observed at 6 hpi, except in the case of r3A-VPg, which was detected at 24 hpi (Fig. 2). A time-course analysis of the proteolytic processing of the NoV MD145-12 strain's ORF1 polyprotein in an *in vitro* coupled transcription and

translation assay identified stable precursors r3A + VPg and rPro + RdRp [4]. In our system, rPro and rRdRp cleavage were fast and efficient, which was in contrast to the results obtained from the *in vitro* translation system [4]. This difference may be due to the lack of cell membranes and/or cell membrane-associated host factors accelerating the cleavage process, although we have no direct proof. Our results indicated that rRdRp was cleaved rapidly inside infected human cells and provided mature functional rRdRp (Fig. 3). We have previously shown that the NoV U201 strain's rRdRp expressed in a recombinant baculovirus expression system (insect cells) had negative-strand synthesis activity [9].

In FCV, the proteolytic cleavage sites, recognized by the virus-encoded protease, that define the borders of the nonstructural proteins were found as E/A, E/D, E/N, E/S. This protease cleaved the p38 rN-terminal precursor protein into p5.6 and p32 at E/A. The U201 rN-terminal protein had rN-terminal protein and rNTPase precursor 73-kDa and 37-kDa bands, respectively, as well as a 33-kDa minor band. The U201 strain had an ED motif at amino acids 79 and 80 from N-terminal methionine. The eighteen GII strains in the database had a PPXPXXED motif at amino acid positions 72 to 80 from U201 N-terminal methionine. This suggested that the NoV GII N-terminal protein could be cleaved by the virus protease. However, U201 proteins were expressed by a vTF7 system that also expressed vaccinia virus protease. Further investigations need to be done to investigate this possibility.

When we transfected with the subgenomic-like RNA construct (pT7U201-ORF23) we observed that rVP1 as well as rVP2 were translated (Fig. 2), suggesting that a re-initiation mechanism may occur, such as that reported for lagoviruses [23]. In contrast, neither rVP1 nor rVP2 was expressed when the full-length construct was used for transfection (Fig. 2), despite the fact that a 2.6-kb subgenomic-like RNA band was detected (Fig. 4b). This result indicates that ORF1 proteins were translated from U201 genomic RNA that was capped by the capping enzyme of the vTF7. However, the subgenomic RNA derived with the pT7U201F construct was not translated for unknown reason(s). The details of the calicivirus genome replication and transcription/translation mechanism still remain unclear, but the translation might require a cap or a cap-like structure, or VPg attached to the 5′ end of the genome and subgenome as reported for FCV [15, 30]. Recently, the interaction of NoV VPg with the translation initiation factor eIF3 has been reported [6], and thus it is possible that the NoV VPg regulates transcription and translation initiation events. In this study, a small amount of the rVPg protein (20 kDa) was detected at 24 hpi. However, a 36-kDa r3A-like + VPg precursor, analogous to the picornavirus 3AB (3A protein + VPg), remained a major product at 24 hpi, and still remained at 48 hpi (data not shown), which was similar to the 3A-like + VPg precursor identified in cell culture studies of FCV and RHDV. Interestingly, poliovirus 3A and its putative precursor 3AB are membrane-associated in infected cells, and cleavage of 3AB to 3A and 3B (VPg) by 3CD *in vitro* requires this membrane environment [32]. VPg is a strongly basic peptide predicted not to bind to the membranes of the RNA replication complex; thus, it was postulated that VPg is delivered to the replication complex in the form of a precursor molecule. In

this study, incomplete digestion between r3A-like and rVPg may have affected the translation efficiency from U201 genomic and subgenomic RNA. This suggested that r3A-like + VPg precursor proteins and cleavage events were important in NoV replication. We have not yet determined whether the rVPg was covalently attached at the 5′ end of the 2.6-kb subgenomic-like RNA and 7.6-kb genomic-like RNA. In addition, we could only investigate the maturation of ORF1 proteins until 72 hpi because of the cytopathic effect of the vTF7. Further studies will be needed to investigate NoV replication, including studies using expression systems without the vaccinia virus.

We found that the 7.6-kb negative-strand genomic-like RNA and the 2.6-kb subgenomic-like RNA were transcribed by the functional viral rRdRp. This was evident from the fact that a disrupted RdRp failed to produce genomic and subgenomic RNA. However, rVP1 and rVP2 were not expressed with the full-length construct but were expressed with a subgenomic-like RNA construct. Following this result, we co-transfected the full-length construct and subgenomic-like RNA construct for providing rVP1 and rVP2 proteins in cells. This resulted in the formation of VLPs morphologically similar to NoV with a buoyant density of 1.271 g/cm^3. EM analysis of a heavier fraction, 1.318 g/cm^3, showed round particles, 20 to 80 nm in diameter. Our results indicated that NoV RNA was incorporated into these round particles but not the VLPs. However, the density of these round particles was lighter than norovirus virions purified from stool, which have a density of 1.39–1.40 g/cm^3 in CsCl. Further studies are needed in order to investigate the possible infectivity of these round particles and to determine if they represent undeveloped VLPs.

Acknowledgements

This work was supported in part by a grant for Research on Emerging and Re-emerging Infectious Diseases, Research on Food Safety from the Ministry of Health, Labor and Welfare of Japan, and a grant for Research on Health Science Focusing on Drug Innovation from The Japan Health Science Foundation.

References

1. Ball JM, Estes MK, Hardy ME, Conner ME, Opekun AR, Graham DY (1996) Recombinant Norwalk virus-like particles as an oral vaccine. Arch Virol [Suppl 12]: 243–249
2. Ball JM, Graham DY, Opekun AR, Gilger MA, Guerrero RA, Estes MK (1999) Recombinant Norwalk virus-like particles given orally to volunteers: phase I study. Gastroenterology 117: 40–48
3. Baric RS, Yount B, Lindesmith L, Harrington PR, Greene SR, Tseng FC, Davis N, Johnston RE, Klapper DG, Moe CL (2002) Expression and self-assembly of norwalk virus capsid protein from venezuelan equine encephalitis virus replicons. J Virol 76: 3023–3030
4. Belliot G, Sosnovtsev SV, Mitra T, Hammer C, Garfield M, Green KY (2003) In vitro proteolytic processing of the MD145 norovirus ORF1 nonstructural polyprotein yields stable precursors and products similar to those detected in calicivirus-infected cells. J Virol 77: 10957–10974

5. Bertolotti-Ciarlet A, Crawford SE, Hutson AM, Estes MK (2003) The 3′ end of Norwalk virus mRNA contains determinants that regulate the expression and stability of the viral capsid protein VP1: a novel function for the VP2 protein. J Virol 77: 11603–11615
6. Daughenbaugh KF, Fraser CS, Hershey JW, Hardy ME (2003) The genome-linked protein VPg of the Norwalk virus binds eIF3, suggesting its role in translation initiation complex recruitment. EMBO J 22: 2852–2859
7. Duizer E, Schwab KJ, Neill FH, Atmar RL, Koopmans MP, Estes MK (2004) Laboratory efforts to cultivate noroviruses. J Gen Virol 85: 79–87
8. Flynn WT, Saif LJ (1988) Serial propagation of porcine enteric calicivirus-like virus in primary porcine kidney cell cultures. J Clin Microbiol 26: 206–212
9. Fukushi S, Kojima S, Takai R, Hoshino FB, Oka T, Takeda N, Katayama K, Kageyama T (2004) Poly(A)- and primer-independent RNA polymerase of norovirus. J Virol 78: 3889–3896
10. Hansman G, Doan LP, Kguyen T, Okitsu S, Katayama K, Ogawa S, Natori K, Takeda N, Kato Y, Nishio O, Noda M, Ushijima H (2004) Detection of norovirus and sapovirus infection among children with gastroenteritis in Ho Chi Minh City, Vietnam. Arch Virol 149: 1673–1688
11. Hansman GS, Katayama K, Maneekarn N, Peerakome S, Khamrin P, Tonusin S, Okitsu S, Nishio O, Takeda N, Ushijima H (2004) Genetic diversity of norovirus and sapovirus in hospitalized infants with sporadic cases of acute gastroenteritis in Chiang Mai, Thailand. J Clin Microbiol 42: 1305–1307
12. Hansman GS, Katayama K, Oka T, Natori K, Takeda N (2005) Mutational study of sapovirus expression in insect cells. Virol J 2: 13
13. Harrington PR, Lindesmith L, Yount B, Moe CL, Baric RS (2002) Binding of Norwalk virus-like particles to ABH histo-blood group antigens is blocked by antisera from infected human volunteers or experimentally vaccinated mice. J Virol 76: 12335–12343
14. Harrington PR, Yount B, Johnston RE, Davis N, Moe C, Baric RS (2002) Systemic, mucosal, and heterotypic immune induction in mice inoculated with Venezuelan equine encephalitis replicons expressing Norwalk virus-like particles. J Virol 76: 730–742
15. Herbert TP, Brierley I, Brown TD (1997) Identification of a protein linked to the genomic and subgenomic mRNAs of feline calicivirus and its role in translation. J Gen Virol 78: 1033–1040
16. Jiang X, Wang M, Graham DY, Estes MK (1992) Expression, self-assembly, and antigenicity of the Norwalk virus capsid protein. J Virol 66: 6527–6532
17. Kageyama T, Kojima S, Shinohara M, Uchida K, Fukushi S, Hoshino FB, Takeda N, Katayama K (2003) Broadly reactive and highly sensitive assay for Norwalk-like viruses based on real-time quantitative reverse transcription-PCR. J Clin Microbiol 41: 1548–1557
18. Kageyama T, Shinohara M, Uchida K, Fukushi S, Hoshino FB, Kojima S, Takai R, Oka T, Takeda N, Katayama K (2004) Coexistence of multiple genotypes, including newly identified genotypes, in outbreaks of gastroenteritis due to Norovirus in Japan. J Clin Microbiol 42: 2988–2995
19. Karst SM, Wobus CE, Lay M, Davidson J, Virgin HWt (2003) STAT1-dependent innate immunity to a Norwalk-like virus. Science 299: 1575–1578
20. Katayama K, Shirato-Horikoshi H, Kojima S, Kageyama T, Oka T, Hoshino F, Fukushi S, Shinohara M, Uchida K, Suzuki Y, Gojobori T, Takeda N (2002) Phylogenetic analysis of the complete genome of 18 Norwalk-like viruses. Virology 299: 225–239
21. Kojima S, Kageyama T, Fukushi S, Hoshino FB, Shinohara M, Uchida K, Natori K, Takeda N, Katayama K (2002) Genogroup-specific PCR primers for detection of Norwalk-like viruses. J Virol Methods 100: 107–114

22. Mochizuki N, Otsuka N, Matsuo K, Shiino T, Kojima A, Kurata T, Sakai K, Yamamoto N, Isomura S, Dhole TN, Takebe Y, Matsuda M, Tatsumi M (1999) An infectious DNA clone of HIV type 1 subtype C. AIDS Res Hum Retrovir 15: 1321–1324
23. Morales M, Barcena J, Ramirez MA, Boga JA, Parra F, Torres JM (2004) Synthesis in vitro of rabbit hemorrhagic disease virus subgenomic RNA by internal initiation on (−)sense genomic RNA: mapping of a subgenomic promoter. J Biol Chem 279: 17013–17018
24. Noel JS, Fankhauser RL, Ando T, Monroe SS, Glass RI (1999) Identification of a distinct common strain of "Norwalk-like viruses" having a global distribution. J Infect Dis 179: 1334–1344
25. Oka T, Katayama K, Ogawa S, Hansman GS, Kageyama T, Ushijima H, Miyamura T, Takeda N (2005) Proteolytic processing of sapovirus ORF1 polyprotein. J Virol 79: 7283–7290
26. Parwani AV, Flynn WT, Gadfield KL, Saif LJ (1991) Serial propagation of porcine enteric calicivirus in a continuous cell line. Effect of medium supplementation with intestinal contents or enzymes. Arch Virol 120: 115–122
27. Pletneva MA, Sosnovtsev SV, Sosnovtseva SA, Green KY (1998) Characterization of a recombinant human calicivirus capsid protein expressed in mammalian cells. Virus Res 55: 129–141
28. Prasad BV, Hardy ME, Jiang X, Estes MK (1996) Structure of Norwalk virus. Arch Virol Suppl 12: 237–242
29. Ramsey-Ewing A, Moss B (1996) Recombinant protein synthesis in Chinese hamster ovary cells using a vaccinia virus/bacteriophage T7 hybrid expression system. J Biol Chem 271: 16962–16966
30. Sosnovtsev S, Green KY (1995) RNA transcripts derived from a cloned full-length copy of the feline calicivirus genome do not require VpG for infectivity. Virology 210: 383–390
31. Taube S, Kurth A, Schreier E (2005) Generation of recombinant Norovirus-like particles (VLP) in the human endothelial kidney cell line 293T. Arch Virol 150: 1425–1431
32. Teterina NL, Rinaudo MS, Ehrenfeld E (2003) Strand-specific RNA synthesis defects in a poliovirus with a mutation in protein 3A. J Virol 77: 12679–12691
33. Wobus CE, Karst SM, Thackray LB, Chang KO, Sosnovtsev SV, Belliot G, Krug A, Mackenzie JM, Green KY, Virgin HWt (2004) Replication of norovirus in cell culture reveals a tropism for dendritic cells and macrophages. PLoS Biol 2: e432
34. Yap CC, Ishii K, Aizaki H, Tani H, Aoki Y, Ueda Y, Matsuura Y, Miyamura T (1998) Expression of target genes by coinfection with replication-deficient viral vectors. J Gen Virol 79 (Pt 8): 1879–1888

Author's address: Dr. Tomoichiro Oka, Department of Virology II, National Institute of Infectious Diseases, Gakuen 4-7-1, Musashi-murayama, Tokyo 208-0011, Japan; e-mail: oka-t@nih.go.jp

Genetic Diversity of Sapovirus in Children, Australia

Grant S. Hansman,* Naokazu Takeda,* Kazuhiko Katayama,* Elise T.V. Tu,†‡ Christopher J. McIver,†‡ William D. Rawlinson,†‡ and Peter A. White†

Sapovirus was detected in 7 of 95 stool specimens from children with gastroenteritis of unknown etiology in Sydney, Australia, from August 2001 to August 2002 and from February 2004 to August 2004, by using reverse transcription–polymerase chain reaction. Sequence analysis of the N-terminal capsid region showed all human sapovirus genogroups.

Sapovirus (SaV), a member of the genus *Sapovirus* in the family *Caliciviridae*, is an etiologic agent of human gastroenteritis. SaV-associated infections can cause both mild and acute gastroenteritis. Symptoms include watery stool, mild and or acute diarrhea, stomach cramps, nausea, and vomiting (*1*). In a recent study, the independent risk factor for SaV gastroenteritis in children was contact with an index case-patient, usually in daycare centers (*2*). The most widely used method of SaV detection is reverse transcription–polymerase chain reaction (RT-PCR), which has high sensitivity and can be used for further genetic analysis (*3,4*). SaV strains can be divided into 5 genogroups (GI, GII, GIII, GIV, and GV), of which GI, GII, GIV, and GV strains infect humans, while GIII strains infect pigs (*5,6*). The 4 human genogroups can be further divided into genotypes (*7*). The purpose of this study was to describe sapovirus-associated infections in Australia.

The Study

We screened stool specimens for SaV by using RT-PCR and described the genetic diversity of virus-positive specimens. A total of 95 stool specimens were collected from children <18 years of age treated for gastrointestinal illness at the Sydney Children's Hospital. Stool specimens were obtained from patients with gastroenteritis of unknown origin despite extensive investigation. These specimens were negative for common foodborne bacterial pathogens (*Salmonella*, *Shigella*, and *Campylobacter*) and enteric viruses (rotavirus, adenovirus, astrovirus, and norovirus) (IDEIA enzyme-linked immunosorbent assay, Dako Cytomation, Ely, UK). The specimens included 67 of 110 specimens obtained from children hospitalized between August 2001 and August 2002 and 28 of 60 specimens from outpatients between February 2004 and August 2004. Specimens were not tested for the presence of SaV if an etiologic agent was already identified (n = 75).

RNA was extracted and purified as described elsewhere (3). Ten microliters of RNA was reverse transcribed by using SuperScript III RNaseH (–) reverse transcriptase according to the manufacture's instructions (Invitrogen, Carlsbad, CA, USA). PCR was conducted by using a nested approach with primers directed against the N-terminal capsid region (*4*). The PCR products were analyzed by 2% agarose gel electrophoresis and visualized by staining with ethidium bromide. PCR-generated amplicons were excised from the gel and purified by using the QIAquick gel extraction kit (Qiagen, Hilden, Germany). Nucleotide sequences were determined by using the terminator cycle sequence kit (version 3.1) and the ABI 3100 Avant sequencer (Perkin-Elmer ABI, Boston, MA, USA). Nucleotide sequences were aligned by using ClustalX, and distances were calculated by using the 2-parameter method of Kimura (*8*). Phylogenetic trees with bootstrap analysis from 1,000 replicas were generated by using the neighbor-joining method as described previously (*8*).

SaV was detected in 7 of 95 stool specimens from children 9 months to 7 years of age with previously unknown causes of acute gastroenteritis. This represented a minimum prevalence of 4.1% (7 of 170 specimens). Sequence analysis showed the presence of all known human SaV genogroups (Figure). Two sequences (strains Sydney31 and Sydney40), which shared ≈99% nucleotide (nt) identity and belonged to genogroup GI, closely matched (>99% nt identity) the Manchester sequence. Three sequences (strains Sydney53, Sydney77, and Sydney4106) that belonged to genogroup GII had 69%–77% nt identity. Sydney4106 had ≈98% nt identity with the Mc10 sequence, Sydney53 had ≈90% nt identity with the C12 sequence, and Sydney77 had ≈99% nt identity with the Bristol sequence.

We recently reported SaV strains Mc10 and C12 as recombinant strains (*7*). Phylogenetic analysis of the nonstructural region (i.e., genome start to capsid start) grouped Mc10 and C12 in 1 GII cluster (*7*), and the structural region (i.e., capsid start to genome end) grouped Mc10 and C12 into distinct GII genotypes (*7*). Evidence suggested that the recombination site occurred at the polymerase and capsid junction in open reading frame 1, as we recently described with recombinant norovirus strains (*9*). Further sequence analysis of the nonstructural region (i.e., 800 nt of the polymerase gene) showed that Sydney4106 had ≈99% nt identity with Mc10, and Sydney53 had ≈92% nt

*National Institute of Infectious Diseases, Tokyo, Japan; †University of New South Wales, Sydney, New South Wales, Australia; and ‡Prince of Wales Hospital, Sydney, New South Wales, Australia